

Electron Impact Ionization of Haloalkanes in Helium Nanodroplets

Shengfu Yang, Scott M. Brereton, Martyn D. Wheeler, and Andrew M. Ellis*[†]

Department of Chemistry, University of Leicester, University Road, Leicester LE1 7RH, U.K.

Received: August 9, 2005; In Final Form: November 16, 2005

Electron impact (EI) mass spectra of a selection of C1–C3 haloalkanes in helium nanodroplets have been recorded to determine if the helium solvent can significantly reduce molecular ion fragmentation. Haloalkanes were chosen for investigation because their EI mass spectra in the gas phase show extensive ion fragmentation. There is no evidence of any major softening effect in large helium droplets (~60 000 helium atoms), but some branching ratios are altered. In particular, channels requiring C–C bond fission or concerted processes leading to the ejection of hydrogen halide molecules are suppressed by helium solvation. Rapid cooling by the helium is not sufficient to account for all the differences between the helium droplet and gas phase mass spectra. It is also suggested that the formation of a solid “snowball” of helium around the molecular ion introduces a cage effect, which enhances those fragmentation channels that require minimal disruption to the helium cage for products to escape.

1. Introduction

Nanodroplets of superfluid liquid helium show some extraordinary physical properties, including extremely low temperatures (0.4 K for ⁴He) and the potential for rapid cooling of molecules embedded in their interior.^{1,2} For chemists, this offers a unique and exciting environment for exploring a variety of phenomena, such as the formation of metastable molecular complexes.³ The rapid cooling rate is the key to producing these unusual complexes, because molecules are almost continuously cooled as they are drawn together by intermolecular forces. This process can result in species being trapped in shallow, long-range minima on the potential energy surface.

It has been suggested that the rapid cooling in helium droplets may also provide a means of achieving “soft” ionization using electron impact (EI). This ionization process releases excess energy, which in some molecular ions leads to extensive fragmentation in normal gas phase EI mass spectra. However, when encased in liquid helium, there is the possibility that the energized ions formed in the initial ionization step may be cooled sufficiently quickly by evaporative loss of helium atoms to prevent, or at least reduce, the degree of fragmentation. If this were shown to be a general effect, helium droplets may have some applications in analytical mass spectrometry.

The first indication that doped helium droplets can lead to softer ionization was reported by Scheidemann et al.⁴ This team added SF₆ to helium droplets with an average size of approximately 3000 helium atoms. When subjected to EI at 65 eV, the mass spectrum was dominated by two peaks which were assigned to SF₅⁺ and SF₆⁺. This was an interesting result because fragmentation is much more extensive in EI ionization of gaseous SF₆, so much so that the parent ion, SF₆⁺, is not seen at all. In fact, subsequent work has shown that the peak attributed to SF₆⁺ was in fact due to the SF₅⁺–H₂O cluster ion, the presence of trace water vapor in the instrument giving rise to this species.⁵ Despite this correction, the work on SF₆ gave impetus to the idea that helium droplets might be capable of softening the EI ionization process.

In a series of slightly later studies, Janda and co-workers investigated the EI ionization of rare gas atoms and NO clusters in helium droplets of various sizes.^{6–8} Evidence for a softer ionization process in helium droplets came from a study of NO dimers.⁶ Fragmentation to NO⁺ + NO was found to be extensive in small helium droplets, a result that matches gas phase findings. However, for the largest droplets studied, consisting of ~15 000 helium atoms, the fragmentation was dramatically reduced. At the same time, it was also found that the probability of the dopant molecule receiving the positive charge is greatly reduced for large helium droplets. This observation can be explained by a simple mechanism, which begins with ionization of a helium atom near the surface of the droplet. The positive hole may then migrate from atom to atom, but after a small number of hops, this process is terminated either by charge localization on the dopant molecule (if encountered) or by formation of He₂⁺. In large helium droplets the increased average distance between the initial site of ionization and the location of the molecule means that the charge is more likely to localize in the form of He₂⁺ before it can reach the dopant. There is therefore clearly a tradeoff between a maximum cooling effect (large droplets) and maximum charge transfer probability (small droplets).

In recent work, Lewis and co-workers have carried out a detailed study of the fragmentation of the triphenylmethanol (TPM) cation in helium droplets.⁹ The EI-induced fragmentation pattern was found to change markedly for TPM in a helium droplet compared with the corresponding gas phase EI mass spectrum. In the gas phase the parent ion is a very minor product, whereas in fairly large helium droplets the parent ion is much more abundant. In line with the earlier conclusions of Janda and co-workers, Lewis et al. found the fractional abundances to be a function of droplet size, with the largest droplets (40 000 helium atoms) producing the most effective quenching of fragmentation. This is the maximum droplet size that gave any detectable charge transfer to the TPM dopant molecules. However, even for these relatively large droplets the

[†] E-mail: andrew.ellis@le.ac.uk. Telephone +44 (0)116 2522138. Fax +44 (0)116 2523789.

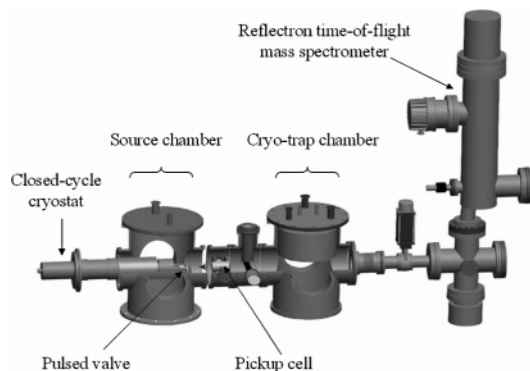


Figure 1. Cross sectional view (to scale) of the experimental apparatus. This apparatus includes a facility for optical spectroscopy experiments between the pickup cell and the cryo-trap chamber that has not been used in the current work.

evidence from concomitant threshold photoelectron-photoion coincidence (TPEPICO) studies is that ion cooling is far from complete.⁹

There is growing interest in the study of the quenching of ion fragmentation processes in helium droplets. However, the work reported to date has focused on a few specific molecules and does not allow for general conclusions about the “hardness” or “softness” of electron impact ionization in doped helium droplets. A wider range of molecules needs to be systematically investigated to answer this question satisfactorily. In this paper we focus on haloalkanes, a class of molecules which have not previously been investigated in helium droplets. Haloalkanes are interesting molecules from a mass spectrometric point of view because their EI mass spectra generally show extensive fragmentation, with facile loss of halogen atoms in particular. This family of molecules therefore provides an opportunity to identify any patterns of ion fragmentation behavior in a helium solvent. In this paper we describe the 70 eV EI mass spectra for a selection of small haloalkanes in helium droplets. We find little evidence for soft ionization of the monomers, but for some of the haloalkanes the distribution of fragment ions is altered. In particular, channels requiring C–C bond fission, or concerted processes leading to the ejection of hydrogen halide molecules, are impeded by the helium matrix. As will be described, we attribute these findings to a cage effect by the helium atoms surrounding the parent ion.

2. Experimental Section

Helium droplets were produced using a pulsed nozzle. Our pulsed nozzle is similar to that employed by Slipchenko and co-workers¹⁰ and consists of a commercial pulsed valve (General Valve series 99) that was modified to allow operation at temperatures as low as 6 K. The stainless steel faceplate of the valve was compression sealed to the valve body using indium wire. A Kel-F poppet was used inside the valve in place of the more commonly used Teflon poppets because the latter have a tendency to crack at very low temperatures.¹¹ The orifice was a 0.5 mm diameter channel drilled fully through the stainless steel faceplate. The valve, cooled by a closed-cycle cryostat, was operated at short opening times of $<200 \mu\text{s}$ and a repetition rate of 10 Hz. Helium droplets were formed by expanding pressurized high purity (99.9999%) helium through the pulsed nozzle and into a vacuum chamber evacuated by a diffusion pump (4600 L s^{-1} pumping speed for helium).

An illustration of the apparatus is presented in Figure 1. The instrument consists of three distinct pumping regions. The droplets formed in the first chamber are skimmed to form a

droplet beam and then enter a second chamber pumped by a 1000 L s^{-1} turbomolecular pump. Just beyond the skimmer is a short (7 cm long) pick-up cell where a controlled amount of dopant gas is added to the droplet beam. The droplets then continue onward into the source region of a reflectron time-of-flight mass spectrometer. Ionization is by a 70 eV pulsed electron beam synchronized to fire on arrival of each helium droplet pulse.

Slipchenko and co-workers determined the average size of the helium droplets produced by their pulsed nozzle by measuring the LIF spectrum of a dopant molecule in the droplets as a function of dopant partial pressure in the pickup cell. Depending on the nozzle conditions (temperature and helium stagnation pressure), average droplet sizes in the range 2×10^4 to 7×10^4 helium atoms were reported. In our experiments we operate at a stagnation pressure of 20 bar and a typical nozzle temperature of 10 K, which according to Slipchenko et al. should give an average droplet size of 50 000 helium atoms. We have independently checked this estimate of the droplet size by recording mass spectra as a function of dopant gas pressure and derive an average droplet size of 60 000 helium atoms, which is close to the Slipchenko value. A pulsed source provides a high flux of relatively large droplets which is excellent for exploring the effect of quenching processes in the limit of large helium droplets.

For the results presented below the partial pressure of the haloalkane in the pickup cell was kept deliberately low to prevent any significant formation of dimers and larger dopant clusters.

3. Results and Discussion

A selection of small saturated haloalkanes were targeted for investigation, as follows.

Halomethanes: dichloromethane, trichloromethane, tetrachloromethane, tribromomethane

Haloethanes: iodoethane, 1,2-dichloroethane, 1,1,2-trichloroethane, 1,1,2,2-tetrachloroethane

Halopropanes: 1,2-dichloropropane, 1,3-dichloropropane

To make a comparison, mass spectra of these molecules were recorded with and without helium droplets. The latter was easily achieved without changing the overall experimental conditions by simply altering the delay between the opening of the pulsed valve and the firing of the electron beam pulse such that the electron beam missed the pulse of helium droplets. For delays that do not sample the helium droplet pulse, the only ion signals were derived from background sample gas drifting from the pickup cell into the mass spectrometer vacuum chamber. These signals were much weaker than those derived from the helium droplet pulse, but with sufficient averaging they were sufficient to establish the gas phase EI mass spectra of the isolated molecules. The gas phase spectra recorded in this work were found to be almost identical with those available in the mass spectral database of the NIST Chemistry Webbook.¹²

The findings for the EI mass spectra of the haloalkane-doped helium nanodroplets are summarized in Table 1 and will now be discussed in detail for each class of compound.

3.1. Halomethanes. For the most part these molecules in helium droplets yielded mass spectra similar to those of the isolated molecule case. The principal fragmentation route for halomethanes is the loss of halogen atoms, with the first halogen atom being particularly easily lost. This is readily understandable in terms of the energetics of the ionization process. The first ionization energy of a helium atom is 24.6 eV, whereas the corresponding values for halomethanes are in the range 10–12

TABLE 1: Summary of Observed Ions and Their Relative Abundances

molecule	ion	<i>m/z</i>	abundance	molecule	ion	<i>m/z</i>	abundance	
dichloromethane	CH ³⁵ Cl ³⁷ Cl ⁺	85	10	1,1,2-tetrachloroethane	C ₂ H ₂ ³⁵ Cl ₄ ⁺	156	<1	
	CH ³⁵ Cl ₂ ⁺	83	14		C ₂ H ₂ ³⁵ Cl ₂ ³⁷ Cl ⁺	133	36	
	CH ₂ ³⁷ Cl ⁺	51	32		C ₂ H ₃ ³⁵ Cl ₂ ³⁷ Cl ⁺	132	21	
	CH ₂ ³⁵ Cl ⁺	49	100		C ₂ H ₃ ³⁵ Cl ₃ ⁺	130	23	
trichloromethane	CH ³⁵ Cl ₃ ⁺	118	<1		C ₂ H ₂ ³⁵ Cl ₃ ⁺	131	40	
	CH ³⁵ Cl ³⁷ Cl ⁺	85	65		C ₂ H ₂ ³⁵ Cl ³⁷ Cl ⁺	98	61	
	CH ³⁵ Cl ₂ ⁺	83	100		C ₂ H ₃ ³⁵ Cl ³⁷ Cl ⁺	97	19	
	C ³⁷ Cl ⁺	49	11		C ₂ H ₂ ³⁵ Cl ₂ ⁺	96	100	
	C ³⁵ Cl ⁺	47	31		C ₂ H ₃ ³⁵ Cl ₂ ⁺	95	31	
tetrachloromethane	C ³⁵ Cl ₄ ⁺	152	<1		1,2-dichloropropane	CH ³⁵ Cl ³⁷ Cl ⁺	85	44
	C ³⁵ Cl ₂ ³⁷ Cl ⁺	119	94			CH ³⁵ Cl ₂ ⁺	83	69
	C ³⁵ Cl ₃ ⁺	117	97			C ₃ H ₆ ³⁵ Cl ³⁷ Cl ⁺	114	5
	C ³⁵ Cl ³⁷ Cl ⁺	84	64	C ₃ H ₅ ³⁵ Cl ³⁷ Cl ⁺		113	12	
	C ³⁵ Cl ₂ ⁺	82	100	C ₃ H ₆ ³⁵ Cl ₂ ⁺		112	^b	
	C ³⁷ Cl ⁺	49	10	C ₃ H ₅ ³⁵ Cl ₂ ⁺		111	15	
tribromomethane	C ³⁵ Cl ⁺	47	25	C ₃ H ₆ ³⁷ Cl ⁺		79	30	
	CH ⁷⁹ Br ⁸¹ Br ₂ ⁺	254	2	C ₃ H ₅ ³⁷ Cl ⁺		78	26	
	CH ⁷⁹ Br ₂ ⁸¹ Br ⁺	252	2	C ₃ H ₆ ³⁵ Cl ⁺		77	90	
	CH ⁸¹ Br ₂ ⁺	175	50	C ₃ H ₅ ³⁵ Cl ⁺		76	89	
	CH ⁷⁹ Br ⁸¹ Br ⁺	173	100	C ₂ H ₄ ³⁷ Cl ⁺		65	10	
	CH ⁷⁹ Br ₂ ⁺	171	51	C ₂ H ₃ ³⁷ Cl ⁺		64	^b	
	CH ⁸¹ Br ⁺	94	36	C ₂ H ₄ ³⁵ Cl ⁺	63	31		
	CH ⁷⁹ Br ⁺	92	37	C ₂ H ₃ ³⁵ Cl ⁺	62	14		
	iodoethane	C ₂ H ₅ I ⁺	156	100	C ₃ H ₆ ⁺	42	69	
		C ₂ H ₄ I ⁺	155	81	C ₃ H ₅ ⁺	41	100	
I ⁺		127	17	C ₃ H ₄ ⁺	40	^b		
C ₂ H ₅ ⁺		29	^a	1,3-dichloropropane	C ₃ H ₆ ³⁵ Cl ³⁷ Cl ⁺	114	7	
C ₂ H ₃ ⁺		27	^a		C ₃ H ₅ ³⁵ Cl ³⁷ Cl ⁺	113	10	
1,2-dichloroethane	C ₂ H ₃ ³⁵ Cl ³⁷ Cl ⁺	99	17		C ₃ H ₆ ³⁵ Cl ₂ ⁺	112	^b	
	C ₂ H ₄ ³⁵ Cl ₂ ⁺	98	24		C ₃ H ₅ ³⁵ Cl ₂ ⁺	111	10	
	C ₂ H ₃ ³⁵ Cl ₂ ⁺	97	13		C ₃ H ₆ ³⁷ Cl ⁺	79	17	
	C ₂ H ₄ ³⁵ Cl ⁺	63	80		C ₃ H ₅ ³⁷ Cl ⁺	78	29	
	C ₂ H ₃ ³⁵ Cl ⁺	62	100		C ₃ H ₆ ³⁵ Cl ⁺	77	58	
	C ₂ H ₂ ³⁵ Cl ⁺	61	28		C ₃ H ₅ ³⁵ Cl ⁺	76	100	
	CH ₂ ³⁷ Cl ⁺	51	13		C ₂ H ₄ ³⁷ Cl ⁺	65	9	
	CH ₂ ³⁵ Cl ⁺	49	38		C ₂ H ₄ ³⁵ Cl ⁺	63	21	
	1,1,2-trichloroethane	C ₂ H ₃ ³⁵ Cl ₂ ³⁷ Cl ⁺	134		10	C ₃ H ₅ ⁺	41	93
		C ₂ H ₂ ³⁵ Cl ₂ ³⁷ Cl ⁺	133		12	C ₃ H ₄ ⁺	40	^b
C ₂ H ₃ ³⁵ Cl ₃ ⁺		132	16 ^b					
C ₂ H ₂ ³⁵ Cl ₃ ⁺		131	10					
C ₂ H ₃ ³⁵ Cl ³⁷ Cl ⁺		99	54					
C ₂ H ₂ ³⁵ Cl ³⁷ Cl ⁺		98	37					
C ₂ H ₃ ³⁵ Cl ₂ ⁺		97	92					
C ₂ H ₃ ³⁵ Cl ₂ ⁺		96	64 ^b					
CH ³⁵ Cl ³⁷ Cl ⁺		85	45					
CH ³⁵ Cl ₂ ⁺		83	47					
C ₂ H ₂ ³⁷ Cl ⁺		63	43					
C ₂ H ₃ ³⁵ Cl ⁺		62	70					
C ₂ H ₂ ³⁵ Cl ⁺		61	100					

^a Contaminant peaks, such as ¹⁴N¹⁵N⁺ at *m/z* = 29, make it difficult to extract meaningful relative intensities for these peaks. ^b These peaks coincide with strong He_{*n*}⁺ cluster peaks and therefore relative intensities have not been determined.

eV.¹² Consequently, when charge exchange occurs, the dopant ion is left with a large amount of excess energy, up to 15 eV. The weakest bonds in the haloalkanes are the carbon–halogen bonds and it is therefore unsurprising that these should be the ones that most readily fission.

Figure 2 provides a typical illustration of our findings for the halomethanes. This shows mass spectra for tribromomethane derived from helium droplets and also in the gas phase in the absence of helium droplets. For the helium droplet spectrum the peaks due to the tribromomethane cation and its fragments are built upon a background of He_{*n*}⁺ cluster ions that progressively decrease in abundance as *n* increases. The cleanliness of the mass spectra in the absence of dopant gas is demonstrated by the spectrum shown in Figure 3. Throughout this paper we show raw spectra rather than attempting to subtract the He_{*n*}⁺ ion contributions, because nozzle pulse-to-pulse intensity fluctuations in the presence and absence of the haloalkane vapor yielded relatively noisy difference spectra.

The dominant organic peaks in both the gas phase and helium droplet spectra in Figure 2 are due to the primary fragment ion, CHBr₂⁺, with only a weak signal from the parent ion. This shows that the surrounding helium atoms are unable to quench the C–Br bond fission in the parent ion to any significant extent. CHBr⁺ is also seen in the helium droplet mass spectrum, with a CHBr⁺/CHBr₂⁺ abundance ratio similar to that in the gas phase. The loss of a second Br atom can occur either by secondary decomposition of CHBr₂⁺ or by loss of Br₂ from the parent ion. Whichever process is dominant, it is again not significantly affected by the helium. In contrast, the minor channel leading to Br⁺ + CHBr₂ is strongly suppressed by the helium matrix. Similar results were found for the other haloalkanes; namely that the carbon–halogen bond fission is almost entirely unaffected by the helium, whereas some higher energy fragmentation channels are significantly affected.

For the halomethanes the threshold energies for producing a cation minus a halogen atom are only marginally above the first

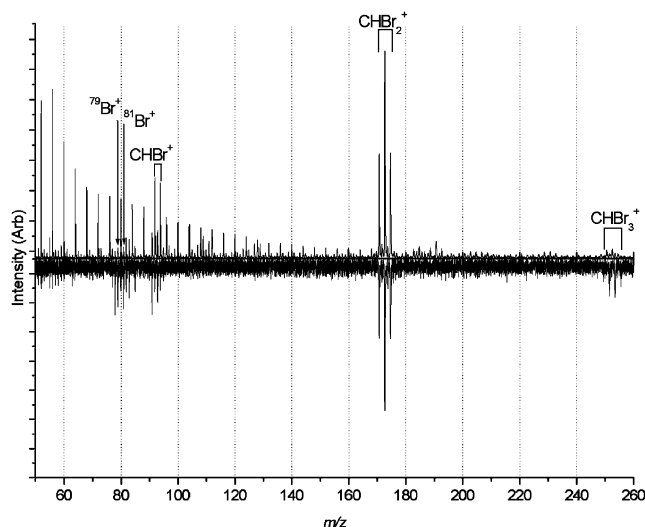


Figure 2. Electron impact (70 eV) mass spectra covering $m/z = 50$ –260 recorded for tribromomethane in helium droplets (upper panel) and the gas phase (helium droplets absent; lower panel). In the helium droplet spectrum the tribromomethane peaks are interspersed between helium cluster peaks, He_n^+ , which are particularly prominent at the low mass end of the spectrum. The increased noise level in the spectrum in the lower panel is due to the low level of “stray” tribromomethane entering the mass spectrometer chamber (see text for further details).

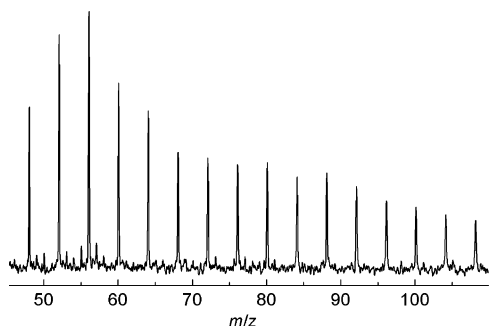


Figure 3. Part of the electron impact ionization mass spectrum for pure helium droplets in the absence of any dopant gas. The spectrum is dominated by peaks due to the He_n^+ cluster ions.

TABLE 2: Enthalpies of Formation and Ionization Energies of Species Derived from CHBr_3

species	$\Delta_f H^\circ / \text{kJ mol}^{-1}$	ionization energy/eV
CHBr_3	55.4 ± 0.02^a	10.50 ± 0.02^a
CHBr_2	201^b	8.3 ± 0.03^a
CHBr	373 ± 17^c	8.90^d
Br_2	30.91 ± 0.11^a	10.517 ± 0.003^a
Br	111.87 ± 0.11^a	11.814^a

^a Data extracted from compilation in ref 12. ^b Calculated value from ref 13. ^c Reference 14. ^d Reference 15.

ionization energy of the halomethane itself. The exact figure varies from molecule to molecule but is typically < 1 eV.¹² Table 2 summarizes the relevant thermochemical and ionization energy data for the case of tribromomethane, and in Table 3 this has been used to calculate appearance energies for the parent and relevant fragment ions. Given the low threshold for CHBr_2^+ formation, it is unsurprising that this ion is seen in abundance: any substantial gain in parent ion at the expense of CHBr_2^+ would imply an exceptional level of rapid cooling by the helium, such that the parent ion is left with very little internal energy. It is worth adding that a gas phase collision-induced dissociation study of the sister ion, CH_2Br_2^+ , shows that even at energies just in excess of the C–Br bond breaking threshold the lifetime

TABLE 3: Appearance Energies^a for Ions Produced from Tribromomethane

appearance energy/eV	ion product	other products
10.5	CHBr_3^+	
11.0	CHBr_2^+	Br
12.5	CHBr^+	Br_2
14.5	CHBr^+	$\text{Br} + \text{Br}$
14.5	Br^+	CHBr_2

^a Derived from the thermochemical mean values listed in Table 2.

of the parent ion is < 100 ns (only an upper limit could be determined).¹⁶ Assuming a similar lifetime applies to CHBr_3^+ , several electronvolts of energy would need to be dissipated on the nanosecond time scale to inhibit the halogen loss channel and the helium droplet mass spectra reported here demonstrate that this does not occur.

More surprising is the fact that the helium does not appear to inhibit the formation of CHBr^+ . The threshold for forming this ion is about 2 or 4 eV above that for formation of the parent ion, depending on whether Br_2 or Br atoms are the products. Interestingly, the channel producing Br^+ is inhibited by the helium matrix. With a formation energy threshold some 4 eV above that of the parent ion, rapid cooling is more feasible as an explanation for the depletion in this channel. However, there are also other possible explanations. Monte Carlo calculations have established that atomic cations in liquid helium attract a solid “snowball” of helium.^{17,18} The layer immediately surrounding the ion behaves like highly compressed solid helium and, for example, shows no indication of any permutational exchange of helium atoms with the second layer of helium atoms (which is also solidlike but has a much lower local density). Because CHBr^+ is a relatively small ion, it will attract a more tightly bound helium inner solvation shell than is the case in larger ions. The stabilizing effect of this shell may provide an additional barrier against escape that is sufficiently large to tip the balance against further carbon–halogen bond fission. Another possibility is that bond fission to produce Br^+ does occur, but this ion is unable to shed all of the helium atoms in the “snowball” as it ploughs through the droplet and escapes into the gas phase. This is a well-known phenomenon in the electron impact ionization of atoms in helium droplets and appears to arise because the atomic ions have no internal energy to dissipate into the surrounding atoms, thereby avoiding evaporative loss of helium atoms.¹⁹ We see no evidence for Br^+He_n cluster ions in the tribromomethane mass spectrum, but it is possible that the range of n is large and therefore that these cluster ions lie beneath the noise level in our mass spectra.

In initiating experiments on the halomethanes in helium nanodroplets, we had anticipated that rapid cooling would allow observation of abundant quantities of parent ions. This is of interest because many halomethane ions, such as CCl_4^+ , are exceptionally difficult to prepare and observe.^{20,21} However, the clear finding from these experiments is that ion dissociation occurs too rapidly for any notable quenching by the helium and the parent ion remains a very minor product.

3.2. Haloethanes. The simplest haloethane investigated was iodoethane. In contrast to the halomethanes, the parent ion is the major product in the 70 eV gas phase mass spectrum of iodoethane, although significant amounts of I^+ , C_2H_5^+ and C_2H_3^+ are also produced. Unsurprisingly, the parent ion remains the most abundant ion in the helium droplet spectrum, but this is almost matched by a strong peak due to $\text{C}_2\text{H}_4\text{I}^+$. The formation of this ion by loss of a single hydrogen atom from the parent ion is barely observable in the gas phase, and so it is

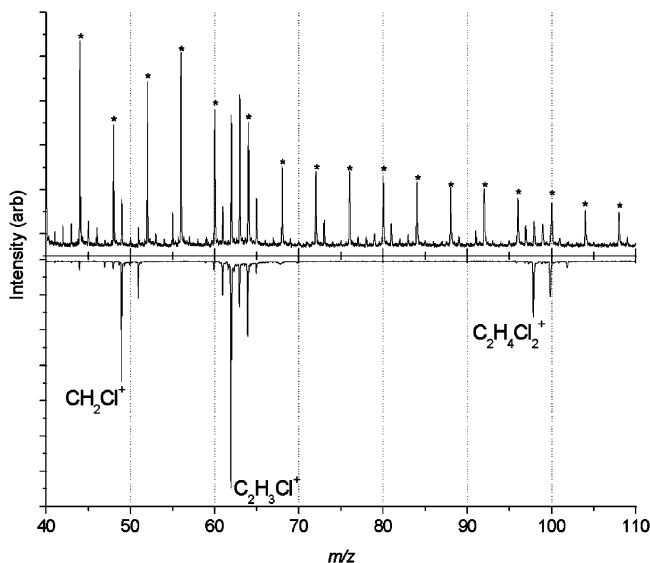


Figure 4. Electron impact mass spectra recorded for 1,2-dichloroethane in helium droplets (upper panel) and in the gas phase (lower panel). Peaks due to He_n^+ cluster peaks are indicated by asterisks. The assignments for chlorine-containing species refer only to the position of the ^{35}Cl isotopomers.

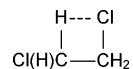
remarkable that this becomes a major product channel in helium droplets. There is insufficient thermodynamic data available in the literature to establish the threshold energy for this process, but it presumably lies above the threshold for C–I bond fission. A cooling effect by the helium is therefore unlikely to account for the appearance of the hydrogen loss channel. In a separate study of the EI mass spectra of alcohols in helium droplets, we have found that hydrogen atom loss channels gain increased prominence in helium droplet mass spectra.²² This finding was attributed to a differential cage effect in which loss of a single hydrogen atom is favored over some molecular elimination channels. The rationale invokes the blocking effect of a tightly bound helium solvation shell, similar to that mentioned earlier for CHBr^+ . The formation of this solvent shell around the parent ion is likely to increase the barrier for fragment escape. Disruption to the solvent layer will be smallest for loss of a single hydrogen atom and we suggest that this is the explanation for the increased branching ratio for this channel in helium droplets when compared with the gas phase.

Matching the findings for the halomethanes, I^+ production from iodoethane is much reduced in helium droplets. It would also have been interesting to comment on the branching ratios for halogen atom loss to form C_2H_5^+ , but this ion clashes with the signal from background $^{14}\text{N}^{15}\text{N}^+$ in the instrument. Frustratingly, deuteration of the precursor would not help to resolve this problem because the region where $m/z < 35$ is congested by various other contaminant peaks, such as $^{16}\text{O}^{18}\text{O}^+$, and so it is difficult to measure branching ratios for ions in this part of the spectrum with any reliability. To gain more information on the carbon–halogen bond fission process, we shift the focus to heavier haloalkanes where this problem does not arise.

The gas phase and helium droplet mass spectra of 1,2-dichloroethane are shown in Figure 4. 1,2-dichloroethane shows some interesting differences between the gas phase and helium droplet mass spectra. In contrast to iodoethane, the parent ion is not the major product in the gas phase EI mass spectrum of 1,2-dichloroethane. Instead, the most abundant ion corresponds to the loss of HCl from the parent ion. It is worth emphasizing that this is very different from the halomethanes, where halogen

atom loss dominates. Halogen atom loss is seen for 1,2-dichloroethane but is a minor channel. After HCl elimination, the most important ion product is CH_2Cl^+ , which is formed by C–C bond fission. The relative abundances of the major product ions in the gas phase spectrum are as follows: $\text{C}_2\text{H}_4\text{Cl}_2^+$ (25), $\text{C}_2\text{H}_4\text{Cl}^+$ (20), $\text{C}_2\text{H}_3\text{Cl}^+$ (100), and CH_2Cl^+ (53).

In the helium droplet spectrum the abundance ratios are altered to the following: $\text{C}_2\text{H}_4\text{Cl}_2^+$ (25), $\text{C}_2\text{H}_4\text{Cl}^+$ (80), $\text{C}_2\text{H}_3\text{Cl}^+$ (100), and CH_2Cl^+ (40). The major difference is the growth in importance of the C–Cl fragmentation relative to the HCl elimination channel. Work by Baer and co-workers on the mechanism of chloroalkane ion fragmentation processes provides a clue to this change between the gas phase and helium droplet mass spectra.^{23–25} In an early PEPICO study Baer showed that HCl elimination from molecules such as chloroethane and dichloroethane is relatively slow, with measured rates for the chloroethane ion lying between 10^5 and 10^7 s^{-1} , depending on the internal energy.²³ In more recent studies combining ab initio calculations with new experimental data, Baer and colleagues have suggested that a quantum tunneling mechanism is necessary to account for the relatively slow rate of HCl elimination.^{24,25} The mechanism proceeds through a four-center transition state of the type



and encounters a barrier to elimination that cannot be exceeded at low ion internal energies.

There is no evidence to suggest that cooling is responsible for the decreased prominence of HCl elimination in our experiments, because this is the lowest energy fragmentation channel of the parent ion and should, if anything, gain in prominence in a helium droplet if cooling was the sole effect in operation. We propose instead that a steric effect resulting from the relatively tight binding of the first helium solvent shell around the parent ion is responsible. The formation of the four-center transition state requires wide-amplitude H–C–C bending motion, but the tightly bound helium layer will obstruct this motion. In addition, the helium solvent may increase both the size and width of any potential barrier, slowing any potential contribution from quantum tunneling. It is interesting to note that a slowing of quantum tunneling in helium nanodroplets compared with the gas phase has already been found for HF and NH_3 dimers.^{26,27} For example, the hydrogen atom interchange tunneling rate was reduced by a factor of 40% for $(\text{HF})_2$ compared with the free gas phase dimer.²⁷ We expect the effect to be even more severe for ions because of the very tightly bound inner helium solvation shell.

1,1,2-Trichloroethane and 1,1,2,2-tetrachloroethane are different from the other two haloethanes studied in this work in that C–C bond fission in the parent ion is a much more important process. For 1,1,2,2-tetrachloroethane this C–C bond breaking turns out to be particularly facile, giving rise to by far the most abundant ion, CHCl_2^+ , in the gas phase spectrum.

Dealing with 1,1,2-trichloroethane first, there is little difference between the gas phase mass spectrum and that recorded in helium droplets. The only significant change is a reduction in the C–C bond fission probability, which yields a modest fall in the CHCl_2^+ intensity relative to the other ion peaks, including the parent ion and the fragment ions $\text{C}_2\text{H}_3\text{Cl}_2^+$ and $\text{C}_2\text{H}_2\text{Cl}^+$.

The changes for 1,1,2,2-tetrachloroethane are more pronounced. In contrast to 1,1,2-trichloroethane, where in the gas phase C–C bond fission is significant but does not correspond

to the major product ion channel, in 1,1,2,2-tetrachloroethane it is C–C bond fission that dominates, i.e.



All other ions, such as those due to sequential Cl atom loss, are minor products, as is the parent ion. In helium droplets we have found that there is partial suppression of C–C bond fission. This is similar to 1,1,2-trichloroethane, although the effect is larger in 1,1,2,2-tetrachloroethane. This shift in the branching ratio away from the C–C bond breaking channel could be due to cooling of the initially excited parent ion by the surrounding helium. However, this seems improbable given that the appearance energy for CHCl_2^+ formation lies barely above that for parent ion formation.¹² Comparison with the findings for all the other haloalkanes discussed earlier suggests that this degree of rapid cooling is unlikely to have taken place. We suggest instead that a more plausible explanation is a cage effect by the surrounding helium atoms. The loss of relatively large primary fragments will require considerable energy to disrupt and escape through the solid helium solvent in the immediate vicinity of the parent ion. This could explain why, in both 1,1,2-trichloroethane and 1,1,2,2-tetrachloroethane, it is only the C–C fission channels that are significantly affected by the helium: the other observed fragmentation channels eject smaller fragments. Furthermore, it also accounts for the effect being greater for tetrachloroethane, because the neutral fragment is larger than in the trichloroethane case.

3.3. Halopropanes. The dominant primary fragmentation process in the gas phase 70 eV electron impact mass spectrum of 1,3-dichloropropane is the loss of HCl. 1,2-Dichloropropane also shows this process, but the most abundant ion in the mass spectrum is $\text{C}_2\text{H}_4\text{Cl}^+$, implying preferential C–C bond fission. The hydrocarbon ions C_3H_5^+ and C_3H_3^+ are also substantial products in the gas phase spectrum. In helium droplets there are substantial changes in relative ion abundances for both dichloropropanes. For 1,2-dichloropropane the C_3H_5^+ and C_3H_3^+ ions are still prominent products but the channel leading to C–C bond fission is notably suppressed. This “quenching” of C–C bond fission parallels that reported above for both 1,1,2-trichloroethane and 1,1,2,2-tetrachloroethane, and as with those two other molecules we tentatively suggest that a cage effect is responsible.

For both 1,2-dichloropropane and 1,3-dichloropropane the fragment ions arising from loss of a single Cl atom gain in intensity relative to the adjacent peaks arising from loss of HCl. This is shown for 1,3-dichloropropane in Figure 5. We can account for this in exactly the same way as already discussed above for 1,2-dichloroethane, namely, that a four-center transition state is required to eliminate HCl whose formation is impeded in the presence of a helium solvation shell.

4. Conclusions

Electron impact mass spectra of haloalkanes in superfluid helium droplets have been recorded for the first time. The extensive fragmentation seen for the isolated molecules in the gas phase is repeated when the molecules are present in helium droplets. However, there are some fragmentation channels that are reduced in importance in helium. These are mainly limited to channels that involve either C–C bond breaking or elimination of hydrogen halides. A cage effect by the surrounding helium can be used to explain why these processes are more strongly influenced than those channels that involve simple

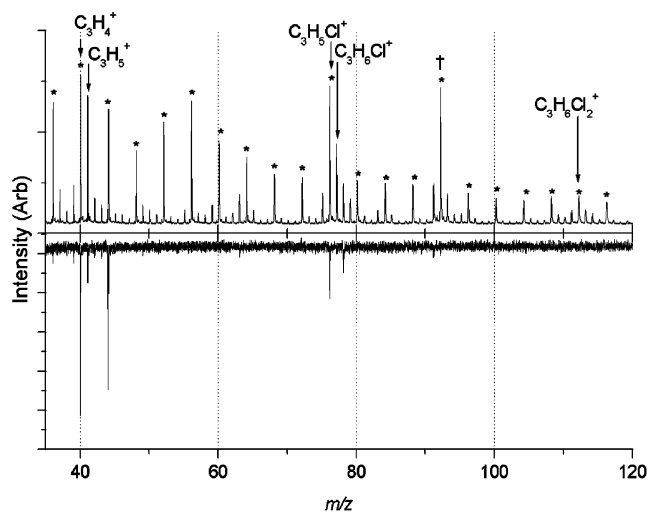


Figure 5. Electron impact mass spectra recorded for 1,3-dichloropropane in helium droplets (upper panel) and in the gas phase (lower panel). Peaks due to He_n^+ clusters are indicated by asterisks, and the single peak at $m/z = 92$ labeled † is due to combined signal from He_{23}^+ and from residual toluene in the vacuum system and inlet line left over from a preceding experiment and which has also been picked up by some helium droplets. The assignments shown for chlorine-containing species are for the ^{35}Cl isotopomers.

elimination of a halogen atom. It is interesting to compare this apparent cage effect with recent findings for the photodissociation of CF_3I in helium nanodroplets.²⁸ In the case of this neutral fragmentation process there is little evidence of any cage effect, with measurements showing that CF_3 fragments emerge from the helium nanodroplets with a speed distribution that is described adequately by a classical collision model. However, a stronger cage effect for cations is plausible given the much stronger interactions between charged species and helium atoms. We hasten to add that we do not at present have any firm evidence for a rigid cage effect and an alternative explanation, involving subtle effects of the helium on the parent ion transition state, must also be considered a possibility. Support from theoretical studies is required to reliably determine the role played by the helium solvent on ion fragmentation and it is hoped that the present work will stimulate interest from theoreticians in this important and interesting problem.

A number of additional experimental studies are planned to build on this initial investigation. This includes recording EI mass spectra of other classes of organic molecules with a wide range of functional groups. In real analytical mass spectrometry any interest in employing helium nanodroplets as an ionization “softener” is likely to focus on large molecules, such as those of potential biological interest, where the avoidance of fragmentation is likely to be of most benefit. With sufficiently large droplet sizes it should be possible to insert detectable amounts of large molecules into helium droplets by modest heating of the analyte sample. Assuming decay rates based on statistical processes, the fragmentation rates of large molecular ions will tend to be much lower than those of small ions such as those studied here. In this case the impact of the helium, and in particular its cooling effect, may be more effective at preventing fragmentation. Evidence for this has recently been found in the study of triphenylmethanol by Miller and co-workers.⁹ We too are also in the process of extending our studies to larger and more complex molecules.

Acknowledgment. We are grateful to the U.K. Engineering and Physical Sciences Research Council for financial support

of this work. We also acknowledge John Weale for his skill and efficiency in constructing the vacuum chambers employed in this work.

References and Notes

- (1) Toennies, J. P.; Vilesov, A. F. *Annu. Rev. Phys. Chem.* **1998**, *49*, 1.
- (2) Toennies, J. P.; Vilesov, A. F. *Angew. Chem. Int. Ed.* **2004**, *43*, 2622.
- (3) Nauta, K.; Miller, R. E. *Science* **2000**, *287*, 293.
- (4) Scheidemann, A.; Schilling, B.; Toennies, J. P. *J. Phys. Chem.* **1993**, *97*, 2128.
- (5) Fröchtenicht, R.; Henn, U.; Toennies, J. P.; Ding, A.; Fieber-Erdmann, M.; Drewello, T. *J. Chem. Phys.* **1996**, *104*, 2548.
- (6) Callicoatt, B. E.; Mar, D. D.; Apkarian, V. A.; Janda, K. C. *J. Chem. Phys.* **1996**, *105*, 7872.
- (7) Callicoatt, B. E.; Förde, K.; Jung, L. F.; Ruchti, T.; Janda, K. C. *J. Chem. Phys.* **1996**, *109*, 10195.
- (8) Ruchti, T.; Förde, K.; Callicoatt, B. E.; Ludwigs, H.; Janda, K. C. *J. Chem. Phys.* **1998**, *109*, 10679.
- (9) Lewis, W. K.; Applegate, B. E.; Sztáray, J.; Sztáray, B.; Baer, T.; Bemish, R. J.; Miller, R. E. *J. Am. Chem. Soc.* **2004**, *126*, 11283.
- (10) Slipchenko, M. N.; Kuma, S.; Momose, T.; Vilesov, A. F. *Rev. Sci. Instrum.* **2002**, *73*, 3600.
- (11) Ghazarian, V.; Eloranta, J.; Apkarian, V. A. *Rev. Sci. Instrum.* **2002**, *73*, 3606.
- (12) *NIST Chemistry WebBook*, <http://webbook.nist.gov>.
- (13) Paddison, S. J.; Tschuikow-Roux, E. *J. Phys. Chem. A* **1998**, *102*, 6191.
- (14) Born, M.; Ingemann, S.; Nibberlung, N. M. *J. Am. Chem. Soc.* **1994**, *116*, 7210.
- (15) Li, Z.; Francisco, J. S. *J. Chem. Phys.* **1998**, *109*, 134.
- (16) Werner, A. S.; Tsai, B. P.; Baer, T. *J. Chem. Phys.* **1974**, *60*, 3650.
- (17) Nakayama, A.; Yamashita, K. *J. Chem. Phys.* **2000**, *112*, 10966.
- (18) Duminuco, C. C.; Galli, D. E.; Reatto, L. *Physica B* **2000**, *284–288*, 109.
- (19) Lewerenz, M.; Schilling, B.; Toennies, J. P. *J. Chem. Phys.* **1995**, *102*, 8191.
- (20) Deutsch, H.; Leiter, K.; Märk, T. D. *Int. J. Mass Spectrom. Ion Processes* **1985**, *67*, 191.
- (21) Hop, C. E. C. A.; Holmes, J. L.; Lossing, F. P.; Terlouw, J. K. *Int. J. Mass Spectrom. Ion Processes* **1988**, *83*, 285.
- (22) Yang, S.; Brereton, S. M.; Wheeler, M. D.; Ellis, A. M. *Phys. Chem. Chem. Phys.* **2005**, *7*, 4082.
- (23) Tsai, B. P.; Werner, A. S.; Baer, T. *J. Chem. Phys.* **1975**, *63*, 4384.
- (24) Morrow, J. C.; Baer, T. *J. Phys. Chem.* **1988**, *92*, 6567.
- (25) Booze, J. A.; Weitzel, K.-M.; Baer, T. *J. Chem. Phys.* **1991**, *94*, 3649.
- (26) Behrens, M.; Buck, U.; Fröchtenicht, R.; Hartmann, M.; Havenith, M. *J. Chem. Phys.* **1997**, *107*, 7179.
- (27) Nauta, K.; Miller, R. E. *J. Chem. Phys.* **2000**, *113*, 10158.
- (28) Braun, A.; Drabbels, M. *Phys. Rev. Lett.* **2004**, *113*, 253401.